

BED TOPOGRAPHY EVOLUTION IN A DISCORDANT BED CHANNEL CONFLUENCE

SEBASTIÁN GUILLÉN LUDEÑA⁽¹⁾, MÁRIO J. FRANCA⁽²⁾,
ANTON J. SCHLEISS⁽³⁾ & ANTÓNIO H. CARDOSO⁽⁴⁾

⁽¹⁾ PhD Student at IST, Lisbon, Portugal / EPFL Lausanne, Switzerland
sebastian.ludena@ist.utl.pt, sebastian.ludena@epfl.ch

⁽²⁾ Research & Teaching Associate, ⁽³⁾ Full Professor, EPFL, Lausanne, Switzerland
mario.franca@epfl.ch, anton.schleiss@epfl.ch

⁽⁴⁾ Full Professor at IST, Lisbon, Portugal
antonio.cardoso@ist.utl.pt

Abstract

Two experimental tests carried out under mobile bed conditions, with different sediment rates in both channels are presented with the aim of studying the bed topography evolution in a discordant bed channel confluence and analyzing the interaction between the bed topography and flow in the confluence. During the tests, bed topography surveys and water level profiles were recorded at the beginning, at equilibrium and at different instants of the experiment. Discharge ratio and flow-morphology interaction were identified as influent factors on the bed topography evolution for both channels.

Keywords: Confluence; Discordant bed; Bed topography evolution; Sediment transport; Morphodynamic.

1. Introduction

During the last century, many river training works were carried out with the aim of satisfying societal needs, i.e. aiming at flood protection, human and industrial water supply or irrigation. Along this process, many environmental aspects were neglected causing several and important impacts on the fluvial ecosystems, mostly through important morphological changes. Nowadays, many tributaries are environmentally disconnected from the main river due to channelization works. To deepen the knowledge of the hydro-morphodynamic processes at these key areas is essential to rehabilitate the original environment at river confluences. The hydrodynamics of river confluences is reasonably well known. Previous studies performed physical and numerical experiments which allowed the development of conceptual models to describe the different flow features observed at confluences. Best (1987) described the flow in river confluences by a scheme in which there are six main zones, corresponding to: flow deflection, flow stagnation, flow separation or recirculation zone, maximum velocity, shear layer and flow recovery zone. Weber et al. (2001) characterized the 3D flow dynamic patterns based on experiments in a 90° confluence channel with fixed and concordant bed. A three-dimensional shape of the flow separation zone (smaller at the bottom) and a warped shear surface were identified for equally wide tributary and main channel.

P. Biron, Best, & Roy (1996) and Bradbrook et al. (2001) analyzed the effects of discordant bed on the flow dynamics at open channel confluences. Their facility consisted of a confluence model with a 30° confluence angle in which the main and tributary channels were 0.12 m and 0.08 m wide respectively. The post-confluence channel was 0.15 m wide to avoid a significant increase in Froude number.

As results of these tests, Biron et al. (1996) concluded by the absence of flow deflection near the bed. Moreover, the discordant bed morphology caused the absence of a flow separation zone at the downstream corner of the confluence and the reduction of the flow acceleration zone in the post-confluence. These last effects created an upwelling flow at the downstream junction corner.

However, few laboratory experiments were carried out under mobile bed conditions. These include the studies of Mosley (1976), Best (1988), Best and Rhoads (2008), Leite Ribeiro (2011) and Leite Ribeiro et al. (2012a; b). Most of the developed morphologic models were based on concordant beds with the exception of Boyer et al. (2006), based on a natural confluence, and Leite Ribeiro (2011) and Leite Ribeiro et al. (2012a; b) who only supplied sediment to the tributary.

Leite Ribeiro et al. (2012a; b) also described the bed morphology of river confluences by five morphological features. These features are bed discordance, which corresponds to the difference between tributary and main-channel bed levels; deposition bar, that is placed along the inner bank downstream of the confluence; avalanche faces of the deposition bar, which constitute the coarse sediment corridor; fine sediment corridor formed on top of the bar near the inner bank; and a slight erosion zone close to the outer bank, associated with the zone of maximum flow velocity.

Based on this conceptual model, Leite Ribeiro et al. (2012a; b) defined the bed discordance as the origin of a two layer flow structure in which tributary flow protrudes in the upper part of the water column of the main channel deflecting the main-channel flow towards the outer bank.

As the bed discordance protects the lowest part of the water column of the main-channel flow from the tributary flow, the main-channel flow deflection only occurs over the upper part of the water column. Hence, the bed discordance inhibits the formation of a zone of horizontal flow recirculation allowing the main-channel flow to move unimpeded downstream.

This paper presents the results of an experimental study on the bed topography evolution in a discordant bed channel confluence where sediments were supplied in both channels.

2. Methodology

Two experimental tests were performed in a laboratory confluence consisting on an 8.5 m long and 0.5 m wide straight glass flume corresponding to the main channel and one PVC channel 4.9 m long and 0.15 m wide channel that corresponds to the tributary, which connects with the main channel 3.60 m downstream its inlet with an angle of 90°. Both channels are rectangular with smooth vertical banks. The results in this paper use the Cartesian coordinates X, Y and Z for the longitudinal, transversal and vertical directions referring to the main channel, as indicated in Figure 1.

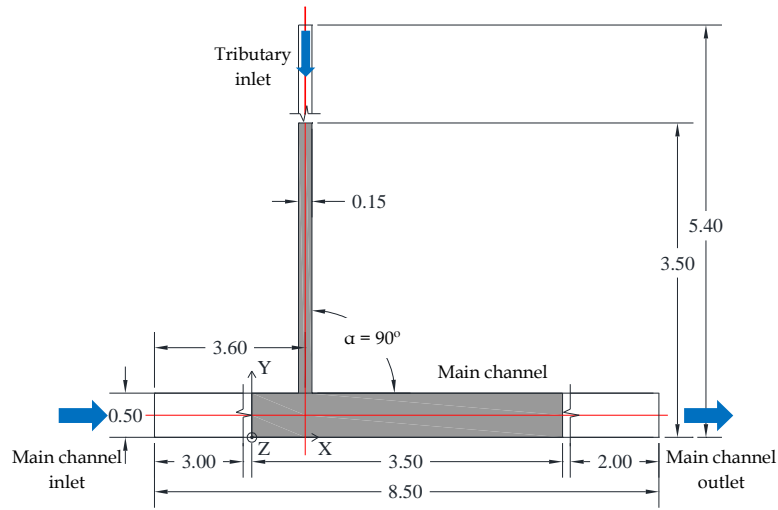


Figure 1. Plan view of the laboratory confluence. The shadow area represents the measurements domain.

Two discharge ratios (Q_r) were tested. The discharge ratio (Q_r) is defined as the ratio between the tributary discharge (Q_t) and the main discharge (Q_m), upstream of the confluence, i.e. $Q_r = Q_t / Q_m$. For all tests, the total post confluence discharge at the (Q_{p-c}) was set to 30 l/s and kept constant (see Table 1). The two scenarios are herein called, intermediate and low.

Table 1. Tested scenarios.

Discharge scenario	Q_t [l/s]	Q_m [l/s]	Q_r [-]	Q_{sm} [kg/min]	Q_{st} [kg/min]
Intermediate	3.9	26.1	0.15	0.30	0.50
Low	3.0	27.0	0.11		

Two types of sediments were supplied during the tests, one at each inlet of both channels (cf. Figure 2 and Table 2). For the tributary, a mixture composed by 80% of 0-4 mm sand and 20% of 4-8 mm gravel was used. This mixture presented a gradation coefficient σ , defined as $\sigma = 0.5 (d_{84}/d_{50} + d_{50}/d_{16})$, of 4.15, corresponding to poorly sorted sediments. For the main channel, the same 0-4 mm sand used for the tributary was used as initial bed material as well as supplied sediment. The gravel part was removed to avoid armoring layer effect in the approach main-channel bed. Table 2 depicts the density value (ρ_s), gradation coefficient (σ), and characteristic sizes where d_m is approached by d_{65} , and d_x is the grain size diameters for which x% of the sediments by weight have smaller diameters. The sieving curves of the sediments for each channel are depicted in Figure 2.

Table 2. Main characteristics of the supplied sediment.

Channel	ρ_s [kg/m ³]	σ [-]	d_{30} [mm]	d_{50} [mm]	d_m [mm]	d_{90} [mm]
Tributary	2650	4.15	0.4	0.8	2.3	5.7
Main channel	2650	3.50	0.4	0.8	1.4	3.0

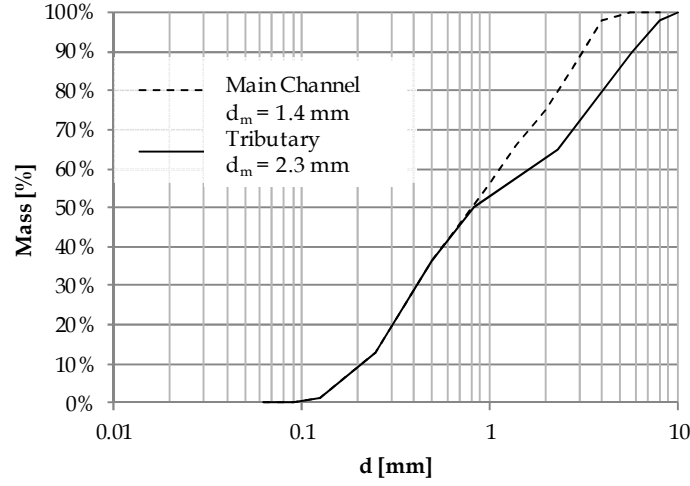


Figure 2. Grain size distribution for supplied sediment into tributary and main channel.

The sediment rates for the tributary and main channel were defined assuming as initial hypothesis that the longitudinal bed slope, and grain size distribution were representative to those observed at the Upper-Rhone River confluences (Leite Ribeiro et al., 2012a; b). Hence, the hypothetical bed slopes were set to 1.0% for the tributary and between 0.3% - 0.4% for the main channel. With these slopes, the defined discharges scenario and assuming uniform flow in both channels, the sediment rates for both channels were estimated using the formula proposed by Smart & Jaeggi (1983) and Smart (1984):

$$Q_b = B_F \times \rho_s \times \frac{4}{s-1} \times R_s \times U \times S^{0.6} \times \left(S - \frac{d_m}{12.1 \times R_s} \right) + \left(\frac{d_{90}}{d_{30}} \right)^{0.2} \quad [1]$$

where Q_b is the sediment transport rate (bed load) in m^3/s , B_F is the width of the flume in m, ρ_s is the sediment density (2650 kg/m^3), s is the relative sediment density ($\rho_s/\rho = 2.65$), ρ is the water density ($\rho = 1000 \text{ kg/m}^3$) R_s is the hydraulic radius in m, U is the mean water velocity in m/s, S is the slope of the channel bed, and d_m , d_{90} , and d_{30} are characteristic grain diameters obtained from the grain size distribution of each type of sediment in m (see Table 2 and Figure 2). This formulation is suitable for the range of diameters and slopes used in the present research and it is widely used in the study of Swiss rivers under similar conditions.

Finally, one constant sediment rate was chosen for each channel from all the computed values. Thus, the adopted sediment rate for the main channel (Q_{sm}) was 0.3 kg/min whereas for the tributary (Q_{st}) was 0.5 kg/min . It was verified later that the adopted sediment rates imposed an equilibrium bed slope close to the hypothesized for each flume.

The channel bed was prepared using different sediment mixtures for each flume; 0-4 mm sand for the main channel and sand-gravel for the tributary. A step of between 0.02 and 0.04 m was made at the junction between main channel and tributary, imposing discordant bed morphology. Also, a longitudinal slope flatter than 1.0% was imposed in the tributary. This bed morphology does not affect to the final topography since, as verified later, the initial slope and the initial step are smaller than those reached in equilibrium.

Once the channel bed was prepared, the model was slowly filled up with water and both bed topographies (tributary and main channel) were measured before the beginning of the tests. By comparing the initial bed surface with the one corresponding to the equilibrium state, scour and deposition areas were later identified.

Water level and bed topography surveys were made after the first 1 and 7 hours of the test, and when the equilibrium was reached. Topography measurements were taken by a Mini-Echo-Sounder ± 1 mm of accuracy. For water level measurements, an ultrasonic limnimeter (± 1 mm accurate) was used.

The tests were run up to reach the equilibrium, i.e. when the ratio between outgoing and incoming sediment discharges was 90% or larger. To check the sediment transport rate at the downstream end, the outgoing sediments were weighted periodically, considering them completely saturated. Additionally, equilibrium was also checked by looking at the evolution of topography surveys.

3. Results and discussions

To analyze the bed topography evolution, three bed longitudinal profiles are herein considered and analyzed in detail for each test, corresponding to the main channel at $Y = 0.05$ and 0.45 m, and to the tributary axis at $X = 0.60$ m (see Figure 3).

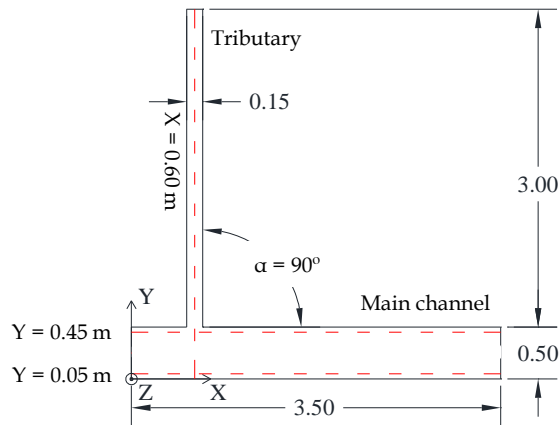


Figure 3. Measurements domain. Red lines represent the analyzed longitudinal profiles.

Figure 4 depicts the bed topography and water surface evolution for the low discharge scenario ($Q_r = 0.11$) by means of the above mentioned profiles.

During the first hour of the test, a scour hole was observed at the tributary mouth (cf Figure 4 b and c). In the meantime, the supplied sediment in the tributary deposited raising the bed level as shown in Figure 4c. The eroded material from the tributary mouth was transported downstream along the inner bank of the main channel (cf. Figure 4b). The bed topography at the outer bank of the main channel did not present remarkable changes during the first hour.

After the first 7 hours of the test, the main channel bed topography presented generalized erosion at the outer bank (cf. Figure 4a) whereas at the inner bank (cf. Figure 4b) a deposition bar began to form with the sediment from the tributary downstream of the confluence.

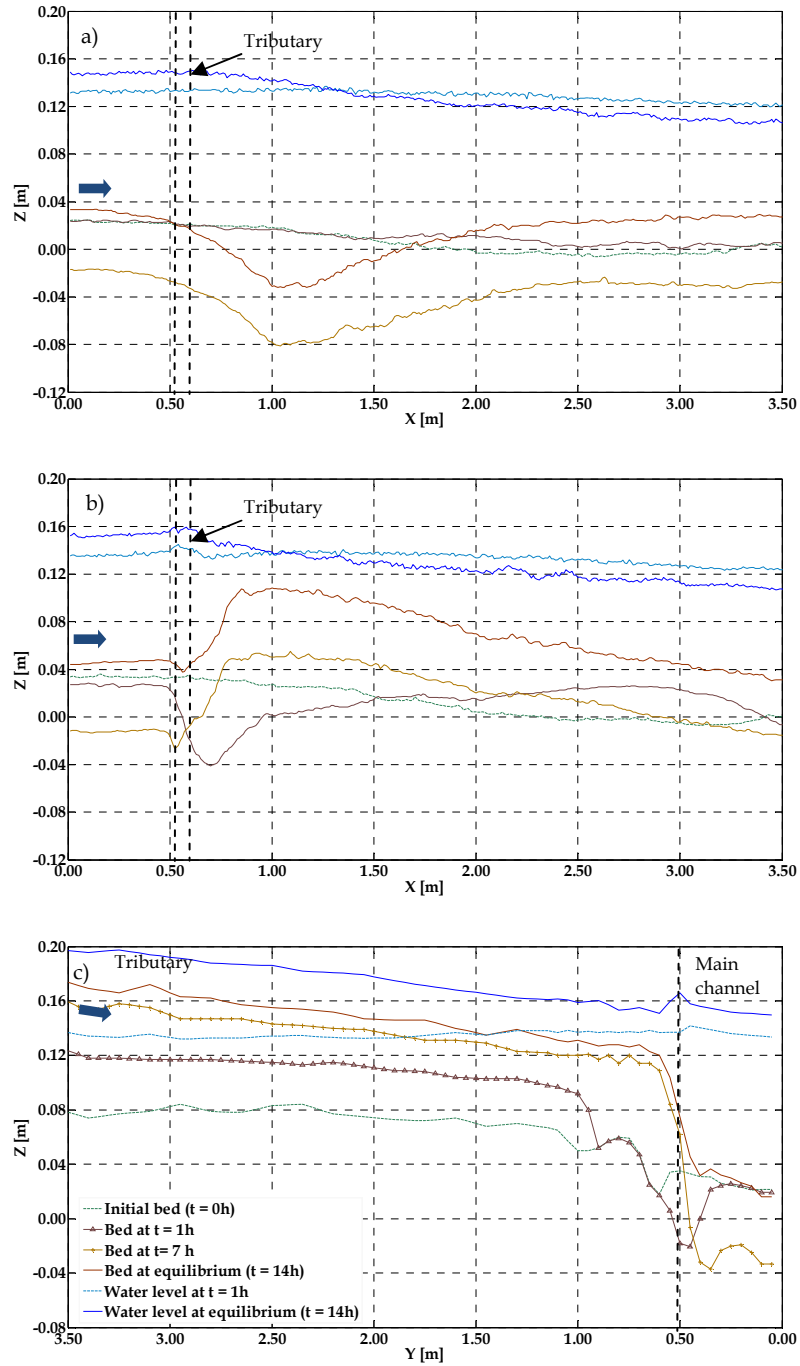


Figure 4. Topography profiles at $t = 0, 1, 7$ and 14 hours of experience, and water level profiles at $t = 1$ h and at equilibrium for the main channel at $Y = 0.05$ m (a) and $Y = 0.45$ m (b) and for the tributary at $X = 0.60$ m (c). Results corresponding to the low scenario ($Q_r = 0.11$).

In the tributary, the supplied sediment kept depositing, raising the bed level and increasing the bed discordance exactly at the junction with the main channel (cf. Figure 4c).

Finally, at equilibrium state the deposition bar was completely developed at the main channel inner bank (cf. Figure 4b) and the sediment supplied by both channels deposited raising the bed level along the main channel as shown in Figure 4a, compared with the state corresponding to 7 h of experience. In the tributary, a slight increase in the bed level was observed during the last 7 hours whereas the bed slope was kept roughly equal. The bed discordance was reduced due to the deposition observed in the main channel (cf. Figure 4c).

Water surface registered an increase of the slope in the main channel downstream of the confluence (cf. Figure 4a and b) due to the reduction of the effective flow section caused by the formation of the deposition bar, which in turn led to a flow acceleration at the outer bank of the main channel. Upstream of the confluence, the water level kept practically the initial water depth and remained practically horizontal due to the backwater curve caused by the tributary inflow. In the tributary, water surface evolved increasing the slope and reducing the water depth, which led to an increase of the flow velocity in the tributary (cf. Figure 4c).

Similar patterns are observed in Figure 5 that represents the results for the intermediate discharge scenario ($Q_r = 0.15$).

After the first hour of the test, a scour hole is also observed at the tributary mouth (Figure 5b and c) but the deposition in the tributary is smaller than that observed for $Q_r = 0.11$. This difference is motivated by the larger transport capacity of the tributary as the discharge in this is larger in the intermediate. Furthermore, in the main channel the deposition bar began to form at the inner bank with the sediment from the tributary, which reduced the effective flow section in the main channel increasing the flow velocity at the outer bank of the main channel eroding the bed (Figure 5a). This erosion at the outer bank of the main channel after 1 hour of test contrasts with the bed topography evolution for the low discharge scenario ($Q_r = 0.11$), where no changes were observed for such period and may be justified by the larger transport capacity of the tributary in the intermediate discharge scenario.

After 7 hours of test duration, the bed topography in the main channel evolved increasing the bed level and the height of the deposition bar at the inner bank (cf. Figure 5b). Deposition was also observed at the outer bank from $X = 0.00$ to 1.00 m (cf. Figure 5a) whereas the erosion is slightly deeper at this bank compared with the observed after 1 hour. On the contrary to the low discharge scenario (Figure 4), where erosion predominated in the main channel after the first 7 hours, for the intermediate discharge scenario, deposition predominated in the main channel. This was reflected on a generalized increase of the bed level in the main channel (cf. Figure 5a) and b). This difference may be justified since the main-channel discharge for the intermediate scenario ($Q_m = 26.1$ l/s) is lower than the discharge corresponding to the low scenario ($Q_m = 27.0$ l/s), whereas for the tributary the discharge changes from $Q_t = 3.0$ l/s for the low scenario to $Q_t = 3.9$ l/s for the intermediate and thus, for the intermediate scenario, the sediment transport capacity is smaller in the main channel and larger in the tributary, compared with the low scenario, which allows larger depositions. In the tributary (Figure 5c), after 7 hours, the bed topography evolved increasing the bed slope, raising the bed level mostly upstream, and filling partially the hole created at the tributary mouth created during the first hour of the test.

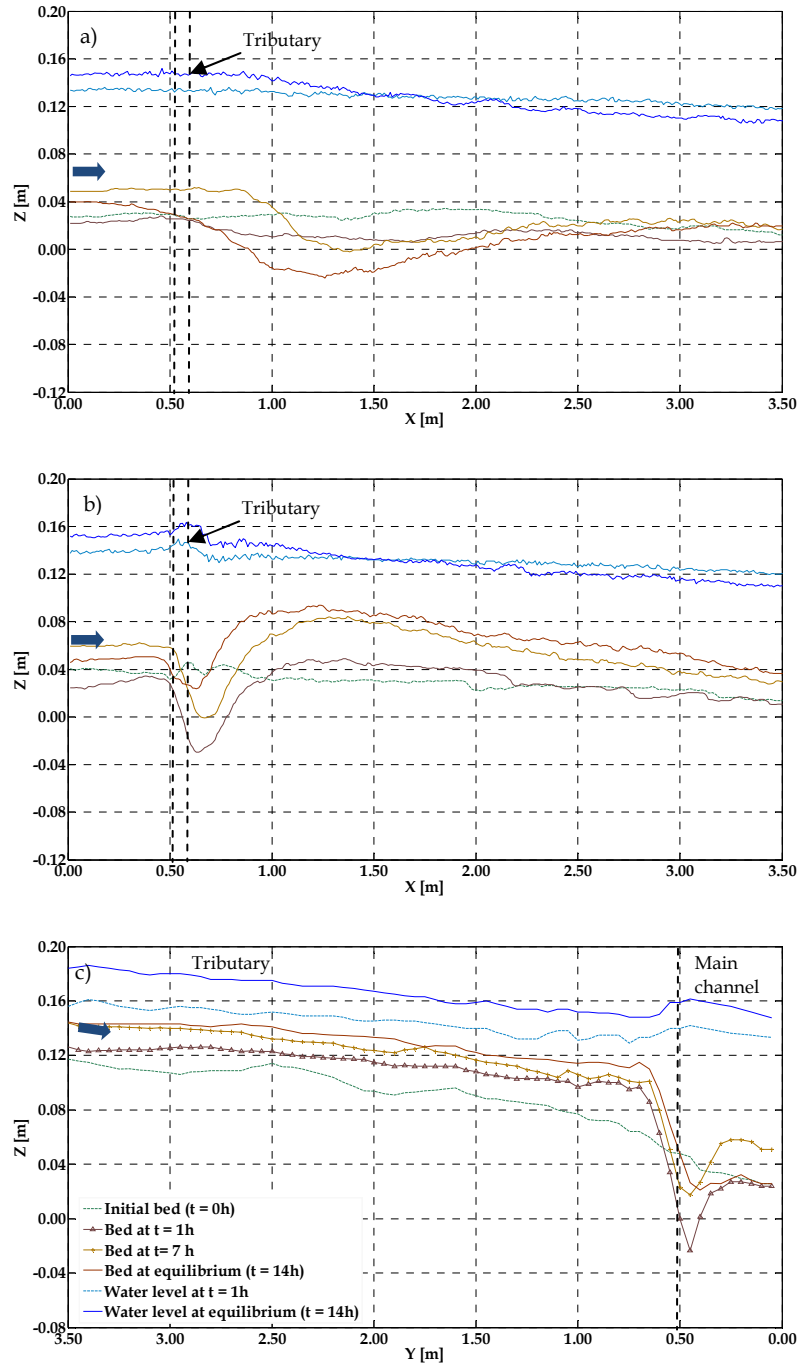


Figure 5. Topography profiles at $t = 0, 1, 7$ and 14 hours of experience, and water level profiles at $t = 1$ and at equilibrium for the main channel at $Y = 0.05$ m (a) and $Y = 0.45$ m (b) and for the tributary at $X = 0.60$ m (c). Results corresponding to the intermediate scenario ($Q_r = 0.15$).

At equilibrium, the deposition bar at the inner bank of the main channel was further developed (cf Figure 5b) whereas at the outer bank, the erosion was deeper and longer than the observed after 7 hours. This erosion was created during the formation of the deposition bar. As the volume of the bar increased, the effective flow section was reduced and the flow at the outer bank was accelerated. The bed topography in the tributary reached the equilibrium increasing slightly the bed level mostly downstream compared to the state at 7 hours.

The evolution of the water surface for this discharge scenario is very close to that observed for the low discharge scenario. The most remarkable difference between this discharge scenario ($Q_r = 0.15$) and that with $Q_r = 0.11$ lay on a smoother change of the water surface slope from the state corresponding to 1 hour and the equilibrium state for $Q_r = 0.15$ (intermediate).

4. Conclusions

Discharge ratio (Q_r) and flow-morphology interaction were identified as influent factors on the bed topography evolution in a mobile bed channel confluence with sediment feeding on both channels.

The discharge ratio directly affects the sediment transport capacity of each channel, influencing the deposition and erosion processes for each channel for a given bed morphology. For instance, the low discharge scenario presented larger depositions in the tributary bed (cf. Figure 4c) for each analyzed period compared with the results observed for the intermediate scenario (cf Figure 5b). In the main channel, for the low discharge scenario ($Q_r = 0.11$), as the main-channel discharge upstream of the confluence ($Q_m = 27$ l/s) is larger than that for the intermediate scenario ($Q_m = 26.1$ l/s), erosion predominating upstream of the confluence during the period between 1 and 7 hour of test experience (cf. Figure 4a), whereas for $Q_r = 0.15$ deposition is observed for the same period in the same region (cf Figure 5a).

Flow-morphology interaction is also an important factor in the bed topography evolution. For both discharge scenarios, the formation of the deposition bar at the inner bank of the main channel is closely related with the observed erosion at the outer bank of the main channel. This erosion is produced by the flow acceleration which, in turn, is caused by the reduction of the effective flow section due to the deposition bar. The erosion at the outer bank of the main channel does not appear until the deposition bar of the inner bank begins to form. This pattern is observed for both discharge configurations in the Figure 4a and b and Figure 5a and b.

Acknowledgments

This research is developed within the framework of the Joint Doctoral Initiative IST-EPFL. Funded by FCT and LCH/EPFL. Contract reference no. SFRH/BD/51453/2011.

References

- Best, J.L., 1987. Flow dynamics at river channel confluences: Implications for sediment transport and bed morphology. *Recent Developments in Fluvial Sedimentology, Spec. Publ. SEPM Soc. Sediment. Geol.*, (39), pp.27-35.
- Best, J.L., 1988. Sediment transport and bed morphology at river channel confluences. *Sedimentology*, 35(3), pp.481-498.

- Best, J.L. & Rhoads, B.L., 2008. Sediment Transport, Bed Morphology and the Sedimentology of River Channel Confluences. In *River Confluences, Tributaries and the Fluvial Network*. John Wiley & Sons, Ltd, pp. 45-72.
- Biron, P., Best, J.L. & Roy, A.G., 1996. Effects of Bed Discordance on Flow Dynamics at Open Channel Confluences. *Journal of Hydraulic Engineering*, 122(12), pp.676-682.
- Boyer, C., Roy, A.G. & Best, J.L., 2006. Dynamics of a river channel confluence with discordant beds: Flow turbulence, bed load sediment transport, and bed morphology. *J. Geophys. Res.*, 111(F4), p.F04007.
- Bradbrook, K.F. et al., 2001. Role of Bed Discordance at Asymmetrical River Confluences. *Journal of Hydraulic Engineering*, 127(5), pp.351-368.
- Leite Ribeiro, M. et al., 2012. Flow and sediment dynamics in channel confluences. *Journal of Geophysical Research: Earth Surface*, 117(F1), pp.1-19.
- Leite Ribeiro, M. et al., 2012. Hydromorphological implications of local tributary widening for river rehabilitation. *Water Resources Research*, 48(10), pp.1-19.
- Leite Ribeiro, M., 2011. Influence of Tributary Widening on Confluence Morphodynamics. *Ecole Polytechnique Fédérale de Lausanne, Lausanne, Switzerland*, 4951.
- Mosley, M.P., 1976. An Experimental Study of Channel Confluences. *The Journal of Geology*, 84(5), pp.535-562.
- Smart, G., 1984. Sediment Transport Formula for Steep Channels. *Journal of Hydraulic Engineering*, 110(3), pp.267-276.
- Smart, G.M. & Jaeggi, M., 1983. Sediment Transport on Steep Slopes. *Mitteilungen der Versuchsanstalt fuer Wasserbau, Hydrologie und Glaziologie, Eidgenossischen Technischen Hochschule, Zurich*, No. 64.
- Weber, L.J., Schumate, E.D. & Mawer, N., 2001. Experiments on flow at a 90 degrees open-channel junction. *J Hydraulic Engineering*, 127(5), pp.340-350.